

Supporting Information

Hydrochar from pine needles as a green alternative for catalytic electrodes in energy applications

A. Marrocchi^{1,*}, E. Cerza¹, S. Chandrasekaran², E. Sgreccia², S. Kaciulis³, L. Vaccaro¹, S. Syahputra⁴, F. Vacandio⁴, P. Knauth⁴, M.L. Di Vona^{2,*}

¹ *University of Perugia, Department of Chemistry, Biology and Biotechnology, via Elce di Sotto 8, 06123 Perugia, Italy*

² *Tor Vergata University of Rome, Dep. Industrial Engineering and International Laboratory: Ionomer Materials for Energy (LIME), 00133 Roma, Italy*

³ *Institute for the Study of Nanostructured Materials, ISMN-CNR, 00015 Monterotondo Stazione, Roma, Italy*

⁴ *Aix Marseille Univ, CNRS, MADIREL (UMR 7246) and International Laboratory: Ionomer Materials for Energy (LIME), Campus St Jérôme, 13013 Marseille, France*

Elemental and proximate analysis

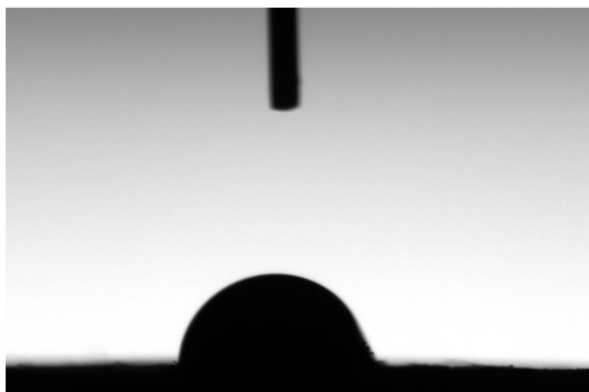
Table S1. Elemental and proximate analysis of pine needles waste

Elemental analysis ^a [wt. %]				
C	H	N	S	O ^c
44.51	5.07	0.47	0.16	48.16
Proximate analysis ^a [wt. %]				
U ^b	VM	Ash	FC ^c	
10.26	84.89	1.63	3.21	

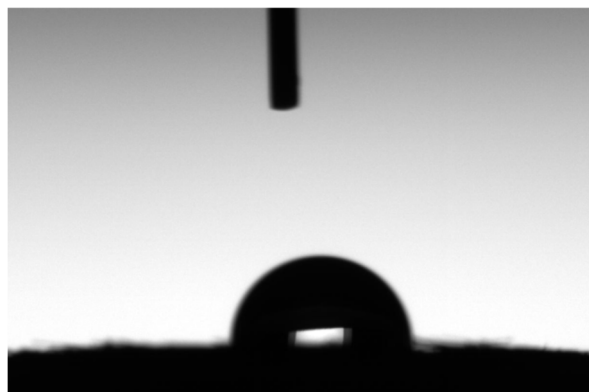
^a Dry basis; ^b Air dry basis; ^c Calculated by difference

Water contact angle

a)



b)



c)

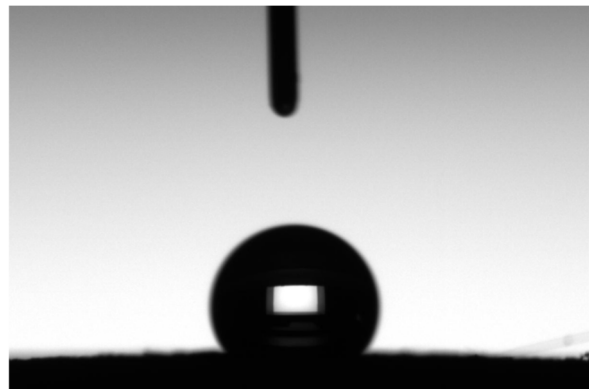


Figure S1. Water contact angle measurements for hydrochar samples: (a) 200_3 ($\Theta = 89^\circ$), (b) 230_1 ($\Theta = 97^\circ$), (c) 260_6 ($\Theta = 129^\circ$).

XPS

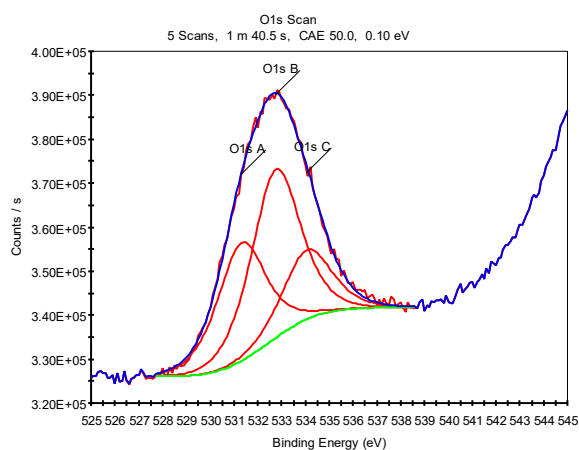


Figure S2. XPS of the O1s region for the sample 200_3. Component A at 531.3 eV –OH, C=O bonded to aromatic carbon; component B at 532.7 eV C-O bonded to aliphatic carbon; component C at 534.1 eV C-O carboxylic.

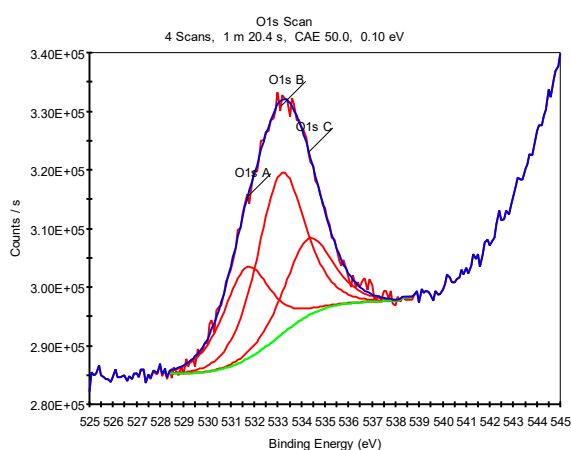


Figure S3. XPS of the O1s region for the sample 230_1. Component A at 531.7 eV –OH, C=O bonded to aromatic carbon; component B at 533.1 eV C-O bonded to aliphatic carbon; component C at 534.3 eV C-O carboxylic.

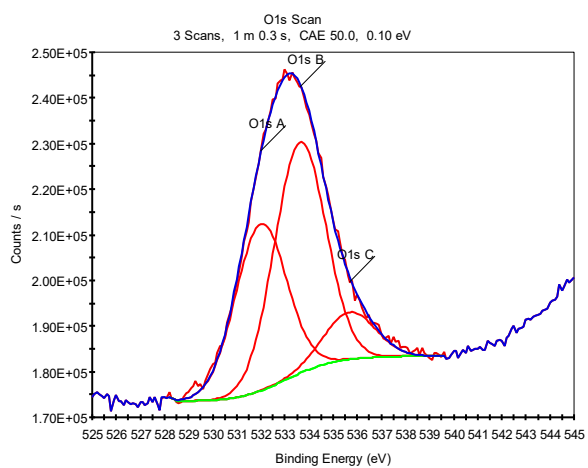


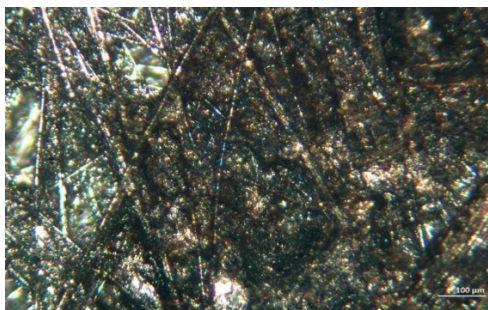
Figure S4. XPS of the O1s region for the sample 260_6. Component A at 532.0 eV –OH, C=O bonded to aromatic carbon; component B at 533.6 eV –C=O, C-O; component C at 535.7 eV –C-O, H₂O.

Optical Micrographs

a)



b)



c)

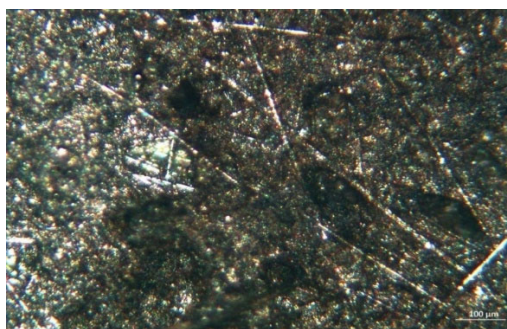


Figure S5. Optical micrographs of hydrochar samples: (a) 200_3, (b) 230_1, (c) 260_6.

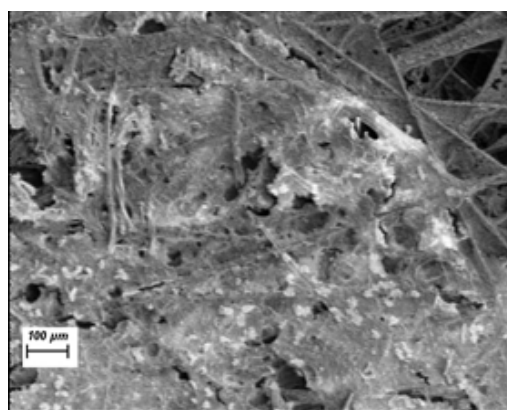
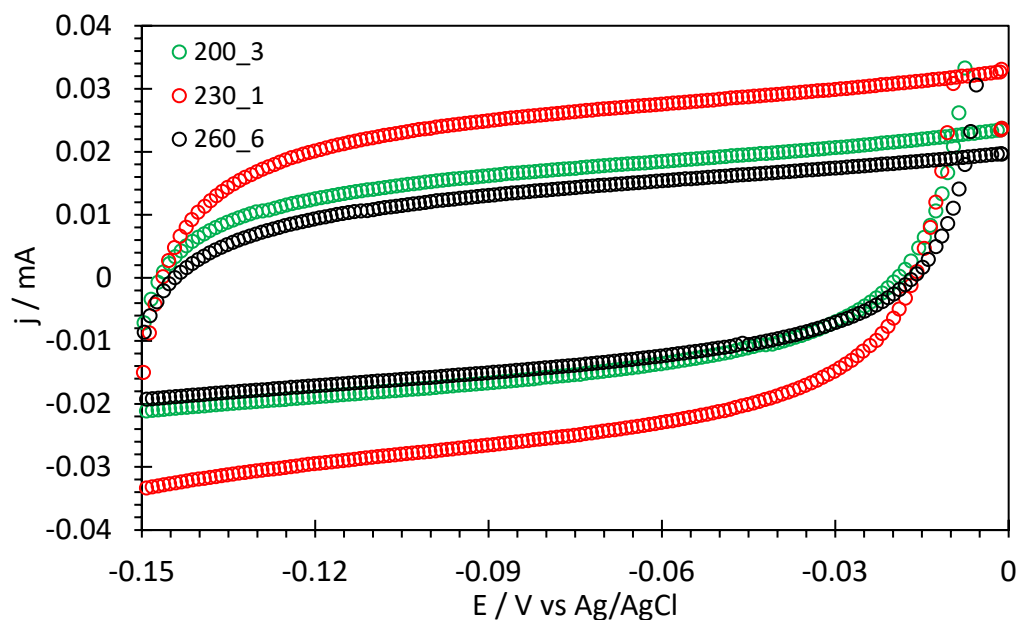


Figure S6. SEM image of hydrochar 230_1.

Electrode Capacitance

a)



b)

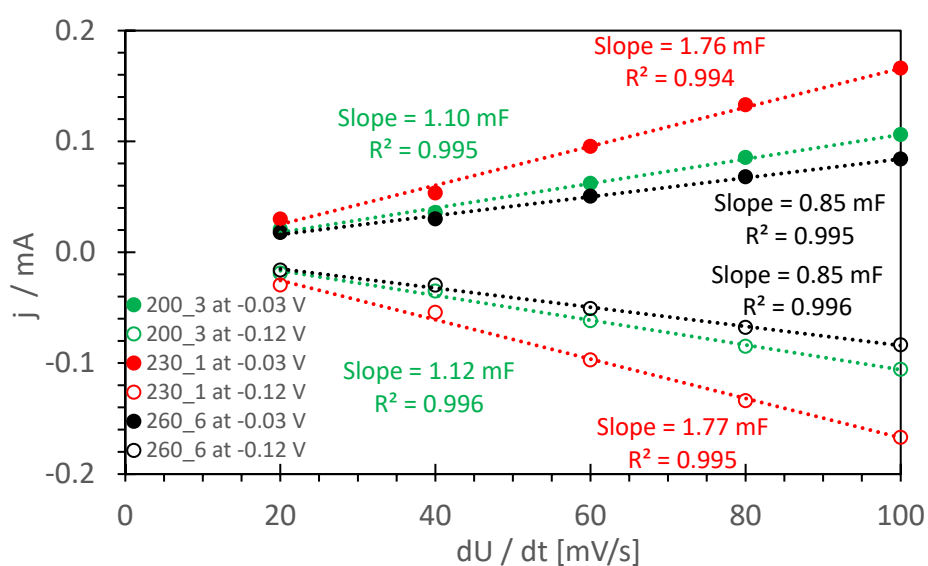


Figure S7. (a) Typical cyclic voltammograms in the non-Faradaic region of hydrochar electrodes in oxygen-saturated 0.1 M KOH solution at 20 mV/s. (b) Determination of the capacitance of electrodes at -0.03 V and -0.12 V vs Ag/AgCl at scan rates 20-100 mV/s according to equation 1.

The electrode capacitance C corresponds to the slope of the non-Faradaic current j as function of the potential scan rate dU/dt :

$$j = C \times dU/dt \quad (S1)$$

The capacitance values C of the hydrochar electrodes are reported in Table S2.

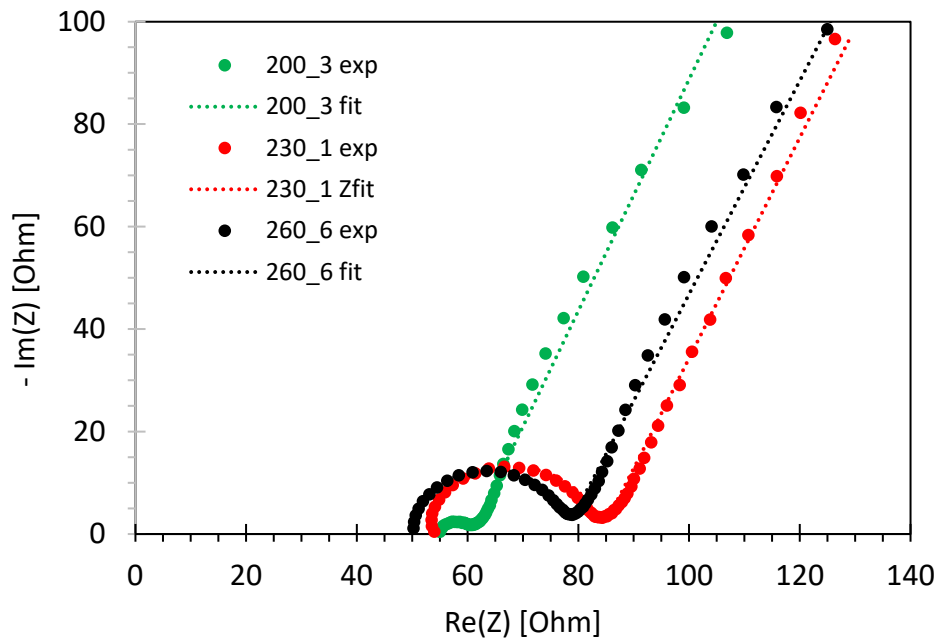


Figure S8. Impedance spectra of hydrochar electrodes in oxygen-saturated 0.1 M KOH solution.

The impedance spectra can be fitted by an equivalent circuit consisting of a resistance $R1$ (representing the electrolyte and electrode resistance), in series with a parallel arrangement of a resistance $R2$ (representing the charge transfer resistance) and a constant phase element $Q2$ (representing the interfacial capacitance) in series with a constant phase element $Q3$ (representing the electrode capacitance) that can be compared with dc capacitance data. The impedance of a constant phase element (CPE) can be written as follows:

$$Z(CPE) = \frac{1}{Q} (i\omega)^{-n} \quad (S2)$$

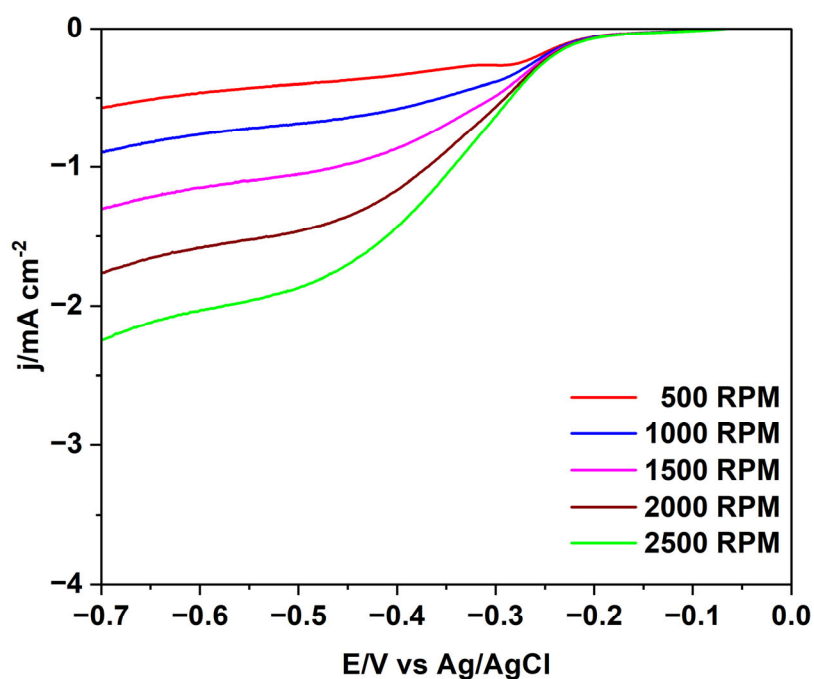
Q is the CPE value and n the CPE exponent; i is the imaginary unit and ω the angular frequency. $n = 1$ relates to an ideal capacitor and $n = 0$ to a pure resistor. $n = 0.5$ is indicative of a diffusion-limited process (Warburg impedance). The non-linear least square-fit data are reported in Table S2.

Table S2. D.c. electrode capacitance C and non-linear least-square fit impedance parameters for hydrochar electrodes.

Sample	C / μF	R_1 / Ω	R_2 / Ω	Q_2 / $\mu F s^{n-1}$	n_2	Q_3 / $\mu F s^{n-1}$	n_3
200_3	1110	54.9	5.8	8.4	0.87	1478	0.73
230_1	1765	52.1	32.0	1.3	0.87	2493	0.72
260_6	850	50.2	27.4	0.6	0.94	1111	0.72

Oxygen reduction reaction (ORR)

a)



b)

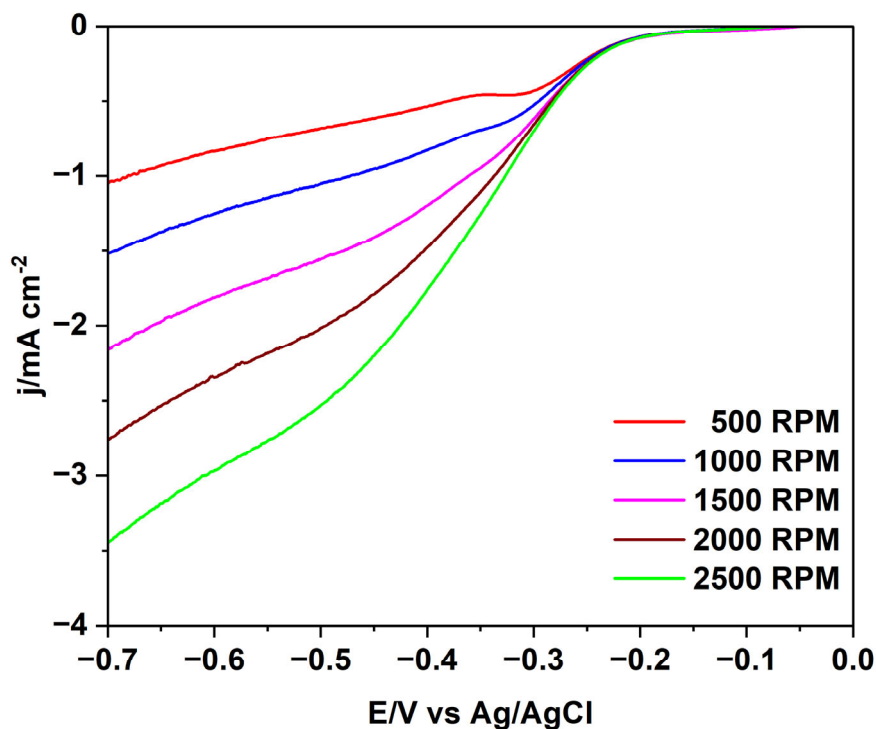


Figure S9. Linear sweep voltammograms for the ORR in oxygen-saturated 0.1 M KOH at various RDE speeds: (a) 200_3 and (b) 260_6 hydrochar electrodes.

The number of exchanged electrons in the ORR can be calculated using the Koutecký–Levich equation:

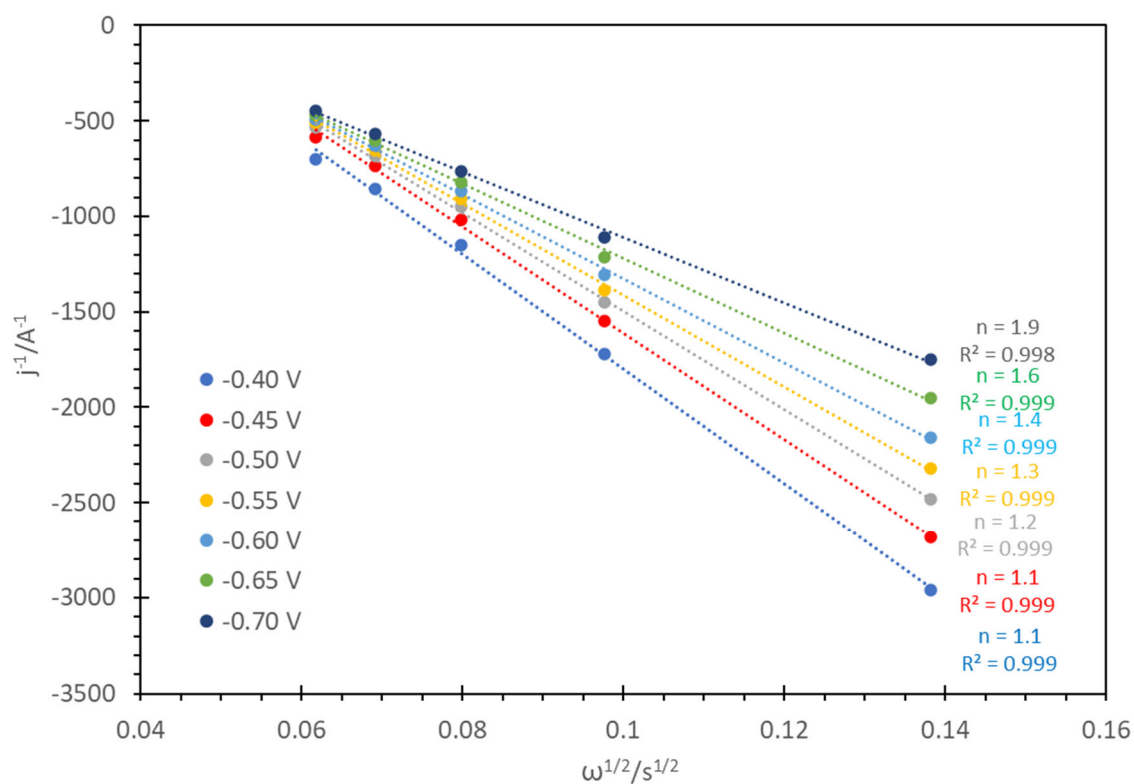
$$\frac{1}{i} = \frac{1}{i^k} + \frac{1}{B \cdot \omega^{\frac{1}{2}}} \quad (\text{S3})$$

i is the limiting current, i^k the kinetic current and ω the angular frequency of the RDE. B is the Levich slope that can be expressed by the equation:

$$B = 0.62 A n F c(O_2) D(O_2)^{\frac{2}{3}} \nu^{\frac{1}{6}} \quad (\text{S4})$$

A is the geometrical electrode area, n the number of exchanged electrons, F the Faraday constant (96485 C mol⁻¹). $c(O_2)$ the saturation concentration of oxygen (1.2 10⁻⁶ mol cm⁻³ in 0.1 M KOH), $D(O_2)$ the oxygen diffusion coefficient (1.9 x 10⁻⁵ cm² s⁻¹ in 0.1 M KOH), and ν the kinematic viscosity (8.7. 10⁻³ cm² s⁻¹ in 0.1 M KOH). Koutecky-Levich plots for the hydrochar 230_1 electrode is reported at various overpotentials in Figure 7 of the main manuscript. The corresponding plots for samples 200_3 and 260_6 can be found in Figure S10.

a)



b)

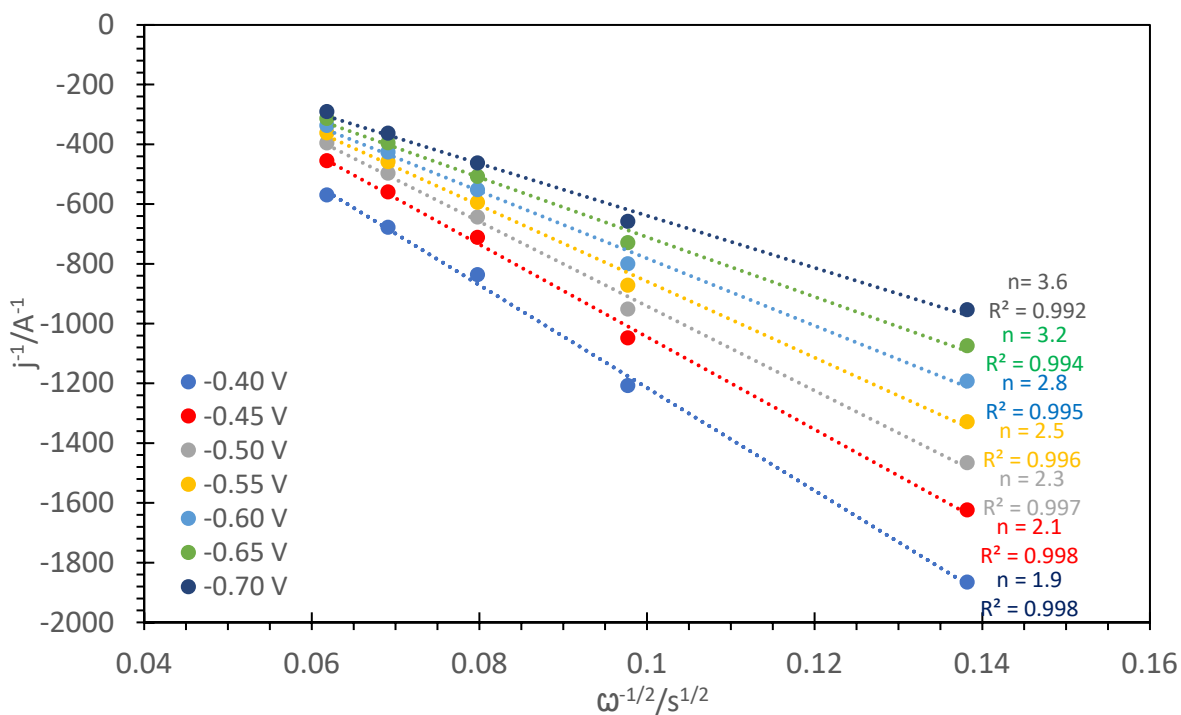


Figure S10. Koutecky-Levich plots at 1500 rpm RDE speed in oxygen-saturated 0.1 M KOH for different electrode potentials (E/V vs Ag/AgCl) for the samples (a) 200_3 and (b) 260_6. The number of exchanged electrons is indicated for each potential.

The Tafel equation between absolute values of the cathodic overpotential $|\eta|$ and the cathodic current density $|i|$ is:

$$|\eta| = \frac{2.3 RT}{\alpha n F} \log\left(\frac{|i|}{i^0}\right) \quad (S5)$$

R is the ideal gas constant, T the absolute temperature, α the symmetry coefficient, n the number of exchanged electrons, F the Faraday constant and i^0 the exchange current density. Figure S11 shows Tafel plots at 1500 rpm for the hydrochar electrodes. A better electrocatalytic activity is generally attributed to a lower slope. The lowest slope of 106 mV/decade for sample 230_1 confirms its better electrocatalytic performance in comparison to other electrodes.

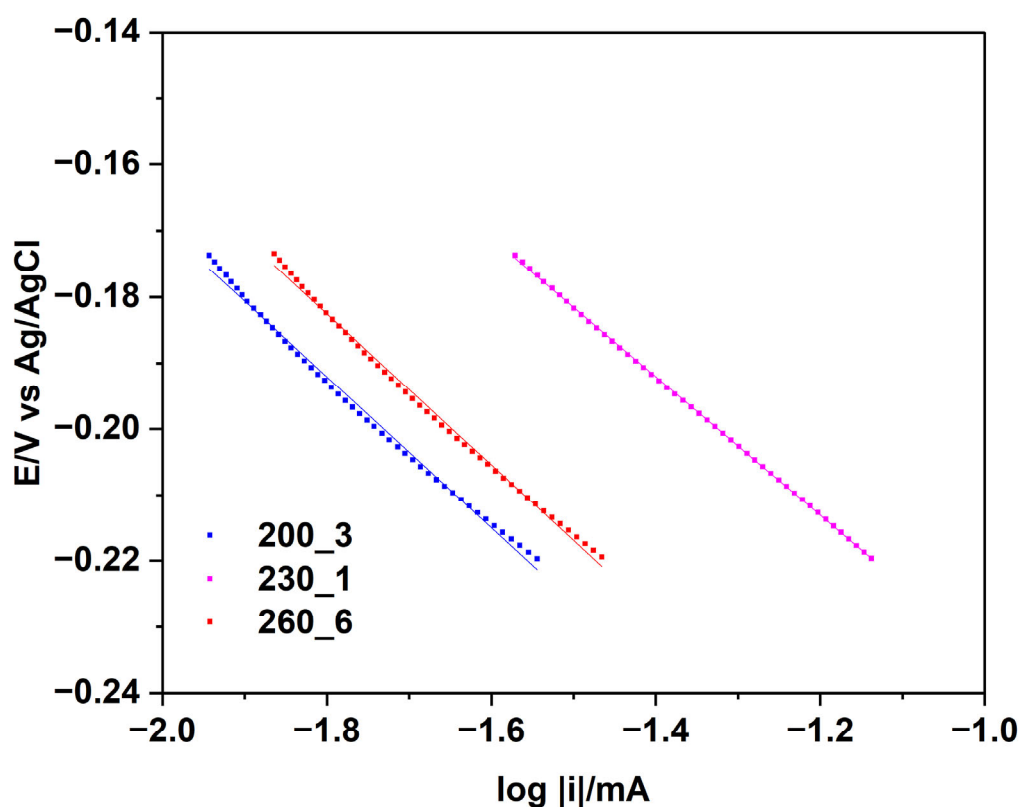
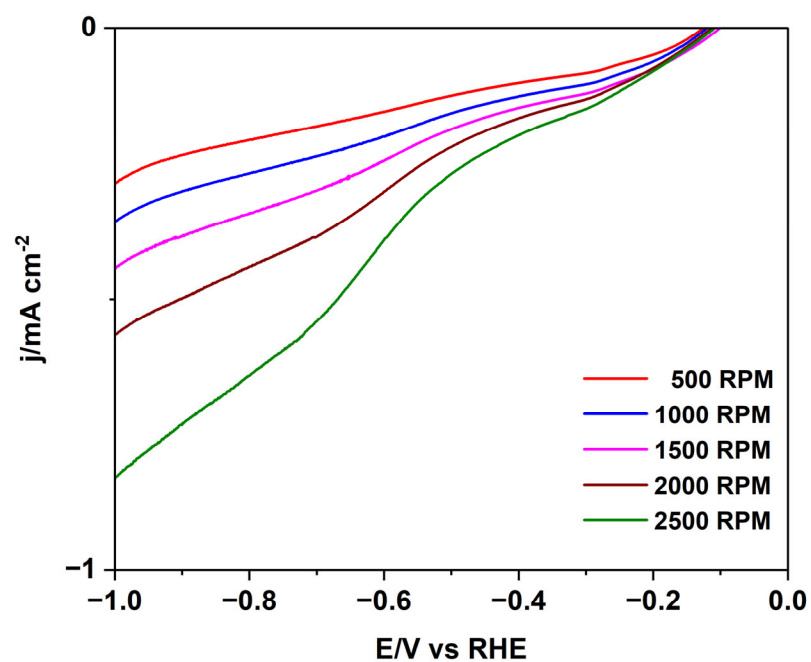


Figure S11. Comparison of Tafel plots of hydrochar electrodes for the ORR in oxygen-saturated 0.1 M KOH at 1500 rpm RDE speed.

CO₂ reduction reaction (CO₂RR)

a)



b)

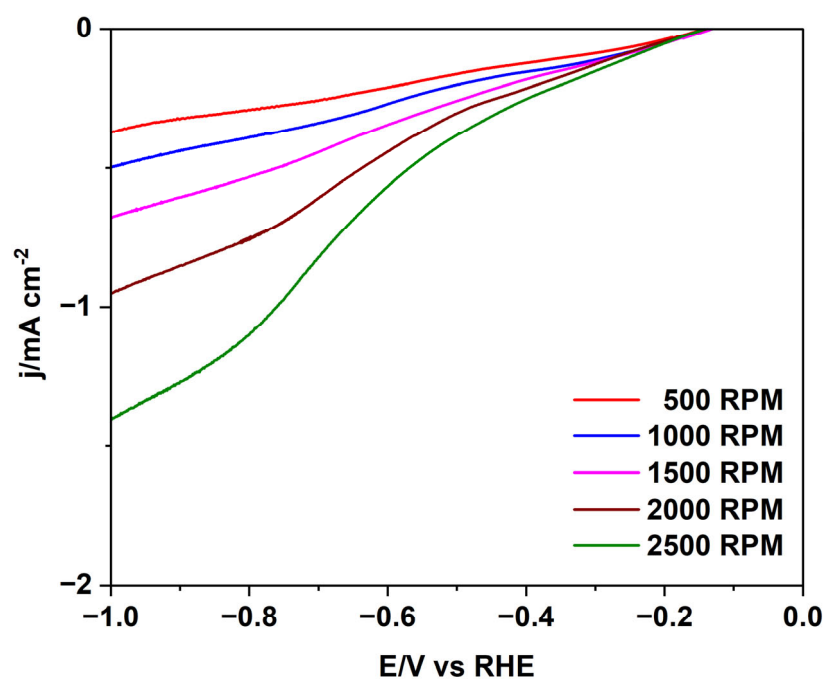


Figure S12. Linear sweep voltammograms for the CO₂RR in CO₂-saturated 0.1 M KHCO₃ at various RDE speeds: (a) 200_3 and (b) 260_6 hydrochar electrodes.